Dislocations and Green's functions in prestressed solids

Luca Prakash Argani

Department of Civil, Environmental & Mechanical Engineering
University of Trento, Italy
in collaboration with
Institute of Mathematical and Physical Sciences
University of Wales, Aberystwyth, UK

07/04/2014

Outline

Summary

- We **generalize** the inclusion and the edge dislocation problems, starting from the solutions given by Eshelby [1–3] and Willis [4], that are limited to the case of linear compressible elasticity.
- The solutions are **extended** to the general case of infinite, homogeneously prestressed and incompressible 2-D elasticity (L.P. Argani, D. Bigoni, and G. Mishuris (2013). "Dislocations and inclusions in prestressed metals". In: Proc. Roy. Soc. A 469 [5]).
- A **new** infinite-body Green's function set is derived for incremental, incompressible, non-linear elastic materials subject to prestress, extending the solutions given in literature (L.P. Argani, D. Bigoni, D. Capuani, and N.V. Movchan (2014). "Cones of localized shear strain in incompressible elasticity with prestress: Green's function and integral representations". *Submitted*).
- Two examples of a circular inclusion and of an edge dislocation dipole have been implemented in order to understand the role of prestress.
- An example of a force dipole in an infinite axisymmetric material shows the formation of conical localization of deformation.

Material defects: preliminaries

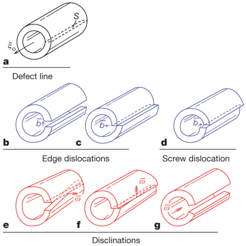

Figure 1: Dislocation classification.

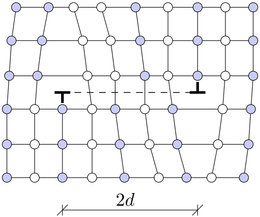

Figure 2: Sketch of the lattice distortion induced by a dislocation dipole.

- A dislocation is a crystallographic defect within a crystal structure, whose presence influences the response of materials.
- Dislocation classification and their influence on the elastic fields have been investigated for the first time by Vito Volterra [6] (figure 1).
- Plastic deformations can be explained in terms of the theory of dislocations.
- In materials science discrete models are adopted, while in continuum mechanics, dislocations are seen as discontinuities.

Material defects: experimental observations and effects of prestress

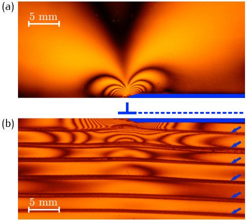

Figure 3: Photoelasticity discloses the stress field around an edge dislocation in isotropic **(a)** and orthotropic **(a)** materials.

Figure 4: Shatter cones beneath meteorite impact craters.

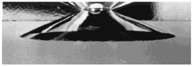

(a) Soda-lime glass.

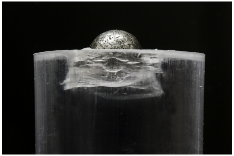

(b) Polycarbonate cylindrical specimen.

Figure 5: Conical fracture produced by a spherical indenter.

- The effect of prestress consists in an induced anisotropy, which has a strong effect on the stress field near inclusions, dislocations, and concentrated forces.

Constitutive framework

- Incompressible non-linear elastic material deformed under plane strain condition.
- **Constitutive equations** (Biot [7]) and **incompressibility** constraint

$$\boxed{\dot{t}_{ij} = \mathbb{K}_{ijkl} v_{l,k} + \dot{p}\delta_{ij} \,, \qquad \mathbb{K}_{ijkl} = \mathbb{K}_{klij} \,, \qquad v_{k,k} = 0 \,.} \tag{1}$$

- **Dimensionless prestress** and **anisotropy parameters** (Bigoni [8])

$$\xi = \frac{\mu_*}{\mu} \,, \qquad \eta = \frac{p}{\mu} = \frac{\sigma_1 + \sigma_2}{2\mu} \,, \qquad \kappa = \frac{\sigma}{2\mu} = \frac{\sigma_1 - \sigma_2}{2\mu} \,. \tag{2}$$

- μ and μ_* are, respectively, the incremental shear moduli parallel to, and inclined at 45° to, the principal stress axes.
- Analysis restricted to the elliptic regime

$$\mu > 0 \,, \qquad \kappa^2 < 1 \,, \qquad 2\xi > 1 - \sqrt{1 - \kappa^2} \,. \tag{3}$$

- Introduction of the J_2-deformation theory of plasticity (Hutchinson & Neale [9])

$$\kappa = \tanh(2\hat{\varepsilon}) \,, \qquad \xi = \frac{N\kappa}{2\hat{\varepsilon}} \,, \qquad \hat{\varepsilon} = \log \lambda \geq 0 \,, \qquad N \in (0, 1) \,. \tag{4}$$

The inclusion problem: preliminaries

- Inclusion of arbitrary shape included in an infinite region (volume D_{in}, surface ∂D_{in}).
- Prescribed uniform incremental displacement gradient $v^{\mathsf{P}}_{i,j}$ that can be thought as an inelastic (e.g. plastic or thermal) deformation.
- The inclusion is constrained by the surrounding matrix material, so that an elastic deformation $v^{\mathsf{E}}_{i,j}$ is produced.

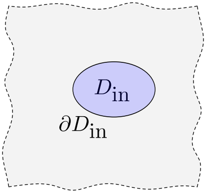

Figure 6: Infinite medium containing an inclusion.

- The 'total' incremental displacement gradient $v_{i,j}$ within the inclusion can be obtained through the additive rule

$$v_{i,j} = v^{\mathsf{E}}_{i,j} + v^{\mathsf{P}}_{i,j}\,. \tag{5}$$

- Although the material is incompressible, v^{P}_{i} *need not satisfy the incompressibility constraint*, so that, since v^{E}_{i} does (namely $v^{\mathsf{E}}_{k,k} = 0$), it follows that $v_{k,k} = v^{\mathsf{P}}_{k,k}$.

The inclusion problem: initial assumptions

- The elastic part of the incremental deformation produces the incremental nominal stress

$$\dot{t}_{ij} = \mathbb{K}_{ijkl} v_{l,k} - \mathbb{K}_{ijkl} v^{\mathsf{P}}_{l,k} + \dot{p}\,\delta_{ij} - \dot{p}^{\mathsf{P}}\delta_{ij}\,. \qquad (6)$$

- $\dot{p}$ and $\dot{p}^{\mathsf{P}}$ are incremental mean stresses, the latter being a homogeneous incremental mean stress, defined inside the inclusion and associated to the deformation $\boldsymbol{v}^{\mathsf{P}}$.
- Neglecting body forces, equilibrium equations for the incremental nominal stress in an infinite body containing a concentrated unit force become

$$\dot{t}^{g}_{ij,i}(\boldsymbol{x}-\boldsymbol{y}) + \delta_{gj}\delta(\boldsymbol{x}-\boldsymbol{y}) = 0\,. \qquad (7)$$

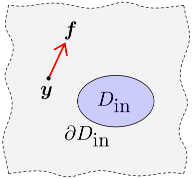

Figure 7: Unit force $\boldsymbol{f}$ applied to a point $\boldsymbol{y}$ of an infinite medium containing an inclusion.

- $\delta(\boldsymbol{x}-\boldsymbol{y})$ is the Dirac delta.
- $\dot{t}^{g}_{ij}$ is the Green's function for incremental nominal stress, in other words, the ij-component of the nominal stress at $\boldsymbol{x}$ produced by a unit point force applied in the g-direction at a point $\boldsymbol{y}$.

The incremental displacement field: the integration domain

- The singularity at point $\boldsymbol{y}$ is enclosed by a disk C_ε centred in $\boldsymbol{y}$, with radius ε and surface ∂C_ε.
- Closed and simply connected domain D_{out} outside both the inclusion and the disk C_ε:

$$D_{\text{out}} = \complement_{\mathbb{R}^n} \{ D_{\text{in}} \cup C_\varepsilon \} \,, \tag{8a}$$

$$\partial D_{\text{out}} = \partial D_{\text{in}} \cup \partial C_\varepsilon \cup \partial D_{\text{ext}} \,, \tag{8b}$$

$n = 2, 3$ for 2-D or 3-D case respectively.

- Betti identity on the region D_{out}:

$$\boxed{\int_{D_{\text{out}}} \left[\dot{t}^g_{ij,i}(\boldsymbol{x}-\boldsymbol{y}) v_j(\boldsymbol{x}) - \dot{t}_{ij,i}(\boldsymbol{x}) v^g_j(\boldsymbol{x}-\boldsymbol{y}) \right] \mathrm{d}V_{\boldsymbol{x}} = 0 \,.} \tag{9}$$

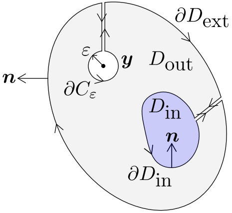

Figure 8: Integration domain for an infinite body containing an inclusion.

Remarks

The comma denotes differentiation with respect to $\boldsymbol{x}$, the same variable for which integration is performed, and $v^g_j(\boldsymbol{x}-\boldsymbol{y})$ is the Green's function for incremental displacements.

The incremental displacement field: the contribution of the sub-regions

- The divergence theorem ($\mathbb{K}_{ijkl} \in \text{Sym}$ and $v_{k,k} = v^g_{k,k} = 0$) leads to

$$\int_{\partial D_{\text{out}}} \left[\dot{t}^g_{ij}(\boldsymbol{x}-\boldsymbol{y}) v_j(\boldsymbol{x}) - \dot{t}_{ij}(\boldsymbol{x}) v^g_j(\boldsymbol{x}-\boldsymbol{y}) \right] n_i \, \mathrm{d}S_{\boldsymbol{x}} = 0 \,. \tag{10}$$

- Since $v^g_i \sim \log r$ (Bigoni & Capuani [10]):

$$\lim_{\varepsilon\to 0} \int_{\partial C_\varepsilon} \dot{t}_{ij}(\boldsymbol{x}) v^g_j(\boldsymbol{x}-\boldsymbol{y}) n_i \, \mathrm{d}S_{\boldsymbol{x}} = 0 \,, \tag{11a}$$

$$\lim_{\varepsilon\to 0} \int_{\partial C_\varepsilon} \dot{t}^g_{ij}(\boldsymbol{x}-\boldsymbol{y}) v_j(\boldsymbol{x}) n_i \, \mathrm{d}S_{\boldsymbol{x}} = v_g(\boldsymbol{y}) \,. \tag{11b}$$

- Assuming that the incremental stress and displacement fields induced by the inclusion decay at infinity, where the outer boundary is moved, and for $\varepsilon \to 0$, we have

$$v_g(\boldsymbol{y}) = \int_{\partial D_{\text{in}}} \left[\dot{t}^g_{ij}(\boldsymbol{x}-\boldsymbol{y}) v_j(\boldsymbol{x}) - \dot{t}_{ij}(\boldsymbol{x}) v^g_j(\boldsymbol{x}-\boldsymbol{y}) \right] n_i \, \mathrm{d}S_{\boldsymbol{x}} \,, \tag{12}$$

where now n_i is the outward unit normal to the inclusion surface ∂D_{in}.

The incremental displacement field

- Since $\dot{p}^{\mathsf{P}}$ is uniform, the integral equation for the incremental displacements outside the inclusion produced by the uniform inelastic field $v^{\mathsf{P}}_{l,k}$ is:

$$v_g(\boldsymbol{y}) = \int_{\partial D_{\text{in}}} \mathbb{K}_{ijkl} v^{\mathsf{P}}_{l,k}(\boldsymbol{x}) v^g_j(\boldsymbol{x}-\boldsymbol{y}) n_i \, \mathrm{d}S_{\boldsymbol{x}} + \int_{D_{\text{in}}} \dot{p}^g(\boldsymbol{x}-\boldsymbol{y}) v^{\mathsf{P}}_{k,k}(\boldsymbol{x}) \, \mathrm{d}V_{\boldsymbol{x}} \,. \tag{13}$$

where $\dot{p}^g(\boldsymbol{x}-\boldsymbol{y})$ is the Green's incremental in-plane mean stress [10].

- If we introduce a potential $P^g_i(\boldsymbol{x}-\boldsymbol{y})$ such that $\dot{p}^g(\boldsymbol{x}-\boldsymbol{y}) = \frac{\partial P^g_i(\boldsymbol{x}-\boldsymbol{y})}{\partial x_i}$, the above equation can be rewritten only in terms of a boundary integral as

$$v_g(\boldsymbol{y}) = \int_{\partial D_{\text{in}}} \left[\mathbb{K}_{ijkl} v^{\mathsf{P}}_{l,k}(\boldsymbol{x}) v^g_j(\boldsymbol{x}-\boldsymbol{y}) + P^g_i(\boldsymbol{x}-\boldsymbol{y}) v^{\mathsf{P}}_{k,k}(\boldsymbol{x}) \right] n_i \, \mathrm{d}S_{\boldsymbol{x}} \,. \tag{14}$$

- Within the 2-D framework, we can obtain a family of potentials $P^g_i(\boldsymbol{x}-\boldsymbol{y})$ in the form

$$P^g_i(\boldsymbol{x}-\boldsymbol{y}) = R_i(\hat{\alpha}) \int \dot{p}^g(\boldsymbol{x}-\boldsymbol{y}) \, \mathrm{d}x_i \,, \qquad R_i(\hat{\alpha}) = \delta_{i1}\hat{\alpha} + (1-\hat{\alpha})\delta_{i2} \,, \tag{15}$$

where the index i is **not** summed, $i, j = 1, 2$ and $\hat{\alpha} \in [0, 1]$.

The incremental displacement field: alternative solutions

- Divergence theorem, incremental equilibrium and the major symmetry of $\mathbb{K}$ in the form

$$\mathbb{K}_{ijkl} v_l^{\mathsf{P}}(\boldsymbol{x}) v^g_{j,ki}(\boldsymbol{x}-\boldsymbol{y}) = -\dot{p}^g_{,l}(\boldsymbol{x}-\boldsymbol{y}) v_l^{\mathsf{P}}(\boldsymbol{x}) \,, \tag{16}$$

lead to an integral equation for the incremental displacements outside the inclusion produced by the uniform inelastic field $v^{\mathsf{P}}_{l,k}$, fully equivalent to (13)

$$\boxed{v_g(\boldsymbol{y}) = \int_{\partial D_{\text{in}}} \left[\mathbb{K}_{ijkl} v^g_{j,i}(\boldsymbol{x}-\boldsymbol{y}) + \dot{p}^g(\boldsymbol{x}-\boldsymbol{y})\delta_{kl}\right] v_l^{\mathsf{P}}(\boldsymbol{x}) n_k \, \mathrm{d}S_{\boldsymbol{x}} \,.} \tag{17}$$

- Green's incremental tractions along the surface of unit normal n_i:

$$\tau^g_j(\boldsymbol{x}-\boldsymbol{y}) = \dot{t}^g_{ij}(\boldsymbol{x}-\boldsymbol{y}) n_i \,, \quad \longrightarrow \quad v_g(\boldsymbol{y}) = \int_{\partial D_{\text{in}}} \tau^g_m(\boldsymbol{x}-\boldsymbol{y}) v^{\mathsf{P}}_m(\boldsymbol{x}) \, \mathrm{d}S_{\boldsymbol{x}} \,. \tag{18}$$

- Expressions for the components of τ^g_j are given both in singular and regularized forms by Bigoni *et al.* [11].

The incremental mean stress field

- Incremental equilibrium equations:

$$\dot{p}_{,j} = -\mathbb{K}_{ijkl} v_{l,ik} \,. \tag{19}$$

- Incremental displacement field (13), (19), and the rate equilibrium equations yield

$$\frac{\partial \dot{p}(\boldsymbol{y})}{\partial y_i} = \int_{\partial D_{\text{in}}} \mathbb{K}_{jklm} v^{\mathsf{P}}_{m,l}(\boldsymbol{x}) \dot{p}^k_{,i}(\boldsymbol{x}-\boldsymbol{y}) n_j \, \mathrm{d}S_{\boldsymbol{x}} - \int_{D_{\text{in}}} \mathbb{K}_{sirg} \dot{p}^g_{,rs}(\boldsymbol{x}-\boldsymbol{y}) v^{\mathsf{P}}_{m,m}(\boldsymbol{x}) \, \mathrm{d}V_{\boldsymbol{x}} \,, \tag{20}$$

and with the other expression (17)

$$\frac{\partial \dot{p}(\boldsymbol{y})}{\partial y_i} = \int_{\partial D_{\text{in}}} \left[\mathbb{K}_{jklm} \dot{p}^k_{,ij}(\boldsymbol{x}-\boldsymbol{y}) - \mathbb{K}_{sirg} \dot{p}^g_{,rs}(\boldsymbol{x}-\boldsymbol{y}) v^{\mathsf{P}}_{m,m} \delta_{lm} \right] v^{\mathsf{P}}_m(\boldsymbol{x}) n_l \, \mathrm{d}S_{\boldsymbol{x}} \,. \tag{21}$$

- Definition of a function $F(\boldsymbol{x}-\boldsymbol{y})$ as

$$F(\boldsymbol{x}-\boldsymbol{y}) = 2\mu^2 \left\{ \left[(1-k)(k+2\xi) - 2\xi^2 \right] v^1_{1,11}(\boldsymbol{x}-\boldsymbol{y}) - k(1+k) v^2_{2,11}(\boldsymbol{x}-\boldsymbol{y}) \right\} , \tag{22}$$

such that [10, Appendix B]

$$\mathbb{K}_{sirg} \dot{p}^g_{,rs}(\boldsymbol{x}-\boldsymbol{y}) = F_{,i}(\boldsymbol{x}-\boldsymbol{y}) \,. \tag{23}$$

The incremental mean stress field

- Integral equation for the incremental mean stress outside the inclusion, produced by the uniform inelastic field $v^{\mathsf{P}}_{l,k}$ using (13):

$$\boxed{\dot{p}(\boldsymbol{y}) = -\int_{\partial D_{\text{in}}} \mathbb{K}_{jklm} v^{\mathsf{P}}_{m,l}(\boldsymbol{x}) \dot{p}^{k}(\boldsymbol{x}-\boldsymbol{y}) n_j \, \mathrm{d}S_{\boldsymbol{x}} + \int_{D_{\text{in}}} F(\boldsymbol{x}-\boldsymbol{y}) v^{\mathsf{P}}_{m,m}(\boldsymbol{x}) \, \mathrm{d}V_{\boldsymbol{x}} \,,} \tag{24}$$

or, using (17),

$$\boxed{\dot{p}(\boldsymbol{y}) = -\int_{\partial D_{\text{in}}} \left[\mathbb{K}_{jklm} \dot{p}^{k}_{,j}(\boldsymbol{x}-\boldsymbol{y}) - F(\boldsymbol{x}-\boldsymbol{y}) \delta_{lm} \right] v^{\mathsf{P}}_{m}(\boldsymbol{x}) n_l \, \mathrm{d}S_{\boldsymbol{x}} \,,} \tag{25}$$

where n_i is the outward unit normal to the inclusion surface ∂D_{in}.

- Incremental nominal stress rate field

$$\dot{t}_{ij}(\boldsymbol{y}) = \mathbb{K}_{ijkl} v_{l,k}(\boldsymbol{y}) + \dot{p}(\boldsymbol{y}) \delta_{ij} \,. \tag{26}$$

Example - The circular inclusion

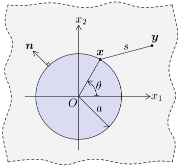

Figure 9: Circular inclusion subject to an inelastic purely volumetric dilatational Eulerian incremental strain $v^{\mathrm{P}}_{i,j} = \beta\delta_{ij}$.

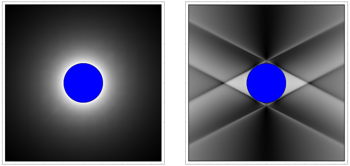

Figure 10: Level sets of $|v_g(\boldsymbol{y})|$ around a circular inclusion. Left: isotropic material without prestress. Right: prestressed J_2-material ($N = 0.363$, $\widehat{\varepsilon} = 0.610$, shear bands inclination at ellipticity loss: $\pm 27.37°$).

- Using the first formulation, (13) and (24):

$$v_g(\boldsymbol{y}) = \mu\beta a \int_0^{2\pi} \left[-(k+\eta)n_1 v_1^g + (k-\eta)n_2 v_2^g\right] \mathrm{d}\theta + \beta\, a^2 \int_0^{2\pi} \dot{p}^g \,\mathrm{d}\theta\,, \tag{27a}$$

$$\begin{aligned}\dot{p}(\boldsymbol{y}) = & -\mu\beta a \int_0^{2\pi} \left[-(k+\eta)n_1 \dot{p}^1 + (k-\eta)n_2 \dot{p}^2\right] \mathrm{d}\theta \\ & + 2\mu^2 \beta\, a^2 \int_0^{2\pi} \left\{ \left[(1-k)(k+2\xi) - 2\xi^2\right] v^1_{1,11} - k(1+k) v^2_{2,11} \right\} \mathrm{d}\theta\,.\end{aligned} \tag{27b}$$

- These equations can be rewritten through the second formulation, (17) and (25).

The edge dislocation dipole

- Thin (thickness h) rectangular inclusion subject to the incremental simple shear displacement field

$$v_i^{\mathrm{P}} = \frac{x_k n_k}{h}\, b_i\,, \qquad b_k n_k = 0\,, \tag{28}$$

  where n_k is the unit vector orthogonal and b_k is a vector parallel to the long edges of the rectangle.

- Inserting equation (28) into the second formulation for the inclusion problem and taking the limit $h \to 0$, we obtain the integral equations for a straight edge dislocation in a prestressed material:

$$\boxed{\begin{aligned} v_g(\boldsymbol{y}) &= \int_L b_m n_l(\boldsymbol{x}) \mathbb{K}_{jklm} v^g_{k,j}(\boldsymbol{x}-\boldsymbol{y})\, \mathrm{d}l_{\boldsymbol{x}}\,, & (29a)\\ \dot{p}(\boldsymbol{y}) &= -\int_L b_m n_l(\boldsymbol{x}) \mathbb{K}_{jklm} \dot{p}^k_{,j}(\boldsymbol{x}-\boldsymbol{y})\, \mathrm{d}l_{\boldsymbol{x}}\,. & (29b)\end{aligned}}$$

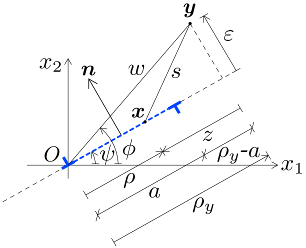

Figure 11: *Edge dislocation dipole* of finite length a and inclined at a constant angle ψ.

Example: level sets of $|v_g(\boldsymbol{y})|$ in an infinite incompressible material

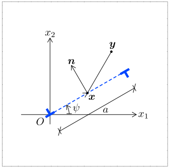

(a) Reference system.

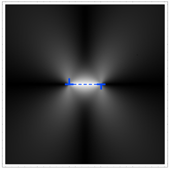

(b) Null prestress.

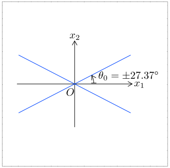

(c) Shear band inclination at ellipticity loss.

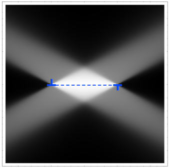

(d) $\psi = 0$.

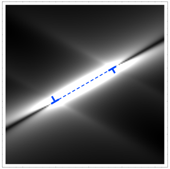

(e) $\psi = \pi/6$.

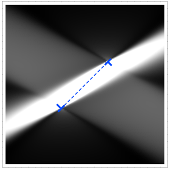

(f) $\psi = \pi/4$.

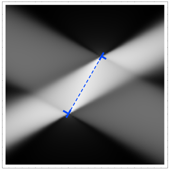

(g) $\psi = \pi/3$.

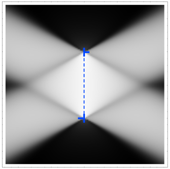

(h) $\psi = \pi/2$.

Figure 12: (b) Classic solution. (d)-(h) Prestressed J_2-material ($N = 0.363$, $\widehat{\varepsilon} = 0.610$).

3-D Green's functions: governing equations

- The general solutions for the inclusion and dislocation problems can be applied to 2-D or 3-D cases: we need the 3-D Green's function for infinite, anisotropic, incompressible, and homogeneously prestressed elasticity.
- Green's stress, equilibrium equations, and incompressibility constraints are

$$\dot{t}^g_{ij} = \mathbb{K}_{ijkl} v^g_{l,k} + \dot{p}^g \delta_{ij}\,, \qquad \dot{t}^g_{ij,i} + \delta_{jg}\delta(\boldsymbol{x}) = 0\,, \qquad v_{k,k} = 0\,. \tag{30}$$

leading to: $\mathbb{K}_{ijkl} v^g_{l,ki} + \dot{p}^g_{,j} + \delta_{jg}\delta(\boldsymbol{x}) = 0.$

- Exploiting plane wave expansion of functions $\delta(\boldsymbol{x})$, $v^g_k(\boldsymbol{x})$, $\dot{p}^g(\boldsymbol{x})$, and introducing the acoustic tensor $A_{jl}(\boldsymbol{\omega}) = \omega_i \mathbb{K}_{ijkl}\omega_k$, in the transformed domain we have

$$\boxed{A_{jl}(\boldsymbol{\omega})\left(\hat{v}^g_l\right)''(\boldsymbol{\omega}\cdot\boldsymbol{x}) + \omega_j\left(\hat{p}^g\right)'(\boldsymbol{\omega}\cdot\boldsymbol{x}) + \delta_{jg}\delta''(\boldsymbol{\omega}\cdot\boldsymbol{x}) = 0\,.} \tag{31}$$

- A manipulation of the incompressibility constraint in the transformed domain yields

$$-\frac{1}{8\pi^2}\int_{|\boldsymbol{\omega}|=1} \omega_k\left(\hat{v}^g_k\right)'(\boldsymbol{\omega}\cdot\boldsymbol{x})\,\mathrm{d}\boldsymbol{\omega} = 0\,, \quad \longrightarrow \quad \omega_k\left(\hat{v}^g_k\right)''(\boldsymbol{\omega}\cdot\boldsymbol{x}) = 0\,. \tag{32}$$

The new infinite-body 3-D Green's function set for anisotropic, incompressible, and homogeneously prestressed elasticity

- Within the elliptic regime $\boldsymbol{A} \in \mathrm{Inv}$ so that we can multiply (31) by $\boldsymbol{A}^{-1}$ and make a projection on $\boldsymbol{\omega}$

$$\omega_k A_{kj}(\boldsymbol{\omega})^{-1} \omega_j \left(\hat{p}^g\right)'(\boldsymbol{\omega}\cdot\boldsymbol{x}) + \omega_k A_{kg}(\boldsymbol{\omega})^{-1} \delta''(\boldsymbol{\omega}\cdot\boldsymbol{x}) = 0\,. \tag{33}$$

- Integration and anti-transform of $\left(\hat{v}_k^g\right)''$ and $\left(\hat{p}^g\right)'$ yield the Green's function set for the 3-D incompressible, anisotropic, prestressed material:

$$v_k^g(\boldsymbol{x}) = -\frac{1}{8\pi^2 r}\int_{|\boldsymbol{\omega}|=1}\left[\frac{A_{kj}^{-1}(\boldsymbol{\omega})\omega_j\omega_t A_{tg}^{-1}(\boldsymbol{\omega})}{\omega_r A_{rs}^{-1}(\boldsymbol{\omega})\omega_s} - A_{kg}^{-1}(\boldsymbol{\omega})\right]\delta(\boldsymbol{\omega}\cdot\boldsymbol{e}_r)\,\mathrm{d}\boldsymbol{\omega}\,, \tag{34a}$$

$$\dot{p}^g(\boldsymbol{x}) = \frac{1}{8\pi^2 r^2}\int_{|\boldsymbol{\omega}|=1}\frac{\omega_k A_{kg}^{-1}(\boldsymbol{\omega})}{\omega_r A_{rs}^{-1}(\boldsymbol{\omega})\omega_s}\delta'(\boldsymbol{\omega}\cdot\boldsymbol{e}_r)\,\mathrm{d}\boldsymbol{\omega}\,. \tag{34b}$$

Implementation technique

- Introduction of an initial $\{\, \boldsymbol{e}_1, \boldsymbol{e}_2, \boldsymbol{e}_3 \,\}$ and a local $\{\, \tilde{\boldsymbol{e}}_1, \tilde{\boldsymbol{e}}_2, \tilde{\boldsymbol{e}}_3 \,\}$ reference system
- **Integral forms** with appropriate description of $\boldsymbol{\omega}$:

$$\int_{|\boldsymbol{\omega}|=1} [\quad]\, d\boldsymbol{\omega} = \int_0^{2\pi}\int_0^{\pi} [\quad] \sin\phi \, d\phi \, d\theta \tag{35}$$

- Treatment of the **incremental displacement field**:

$$\int_{|\boldsymbol{\omega}|=1} [\quad]\delta(\boldsymbol{\omega}\cdot\boldsymbol{x})\, d\boldsymbol{\omega} = \int_0^{2\pi} [\quad]\, d\theta \tag{36}$$

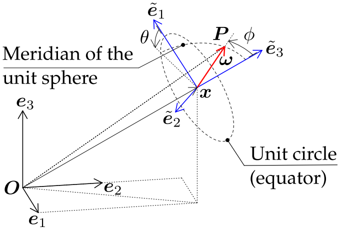

Figure 13: Reference system used for the implementation of the 3-D Green's function set.

- Treatment of the **incremental mean stress field**:

$$\int_{|\boldsymbol{\omega}|=1} g(\boldsymbol{\omega})\delta'(\boldsymbol{\omega}\cdot\boldsymbol{e}_r)\, d\boldsymbol{\omega} = \int_0^{2\pi}\int_0^{\pi} g\big(\boldsymbol{\omega}(\phi,\theta)\big)\delta'(\cos\phi)\sin\phi\, d\phi\, d\theta =$$

$$= \int_0^{2\pi}\int_0^{\pi} -g\big(\boldsymbol{\omega}(\phi,\theta)\big)\frac{\partial\delta(\cos\phi)}{\partial\phi}\, d\phi\, d\theta = \int_0^{2\pi} \left.\frac{\partial g\big(\boldsymbol{\omega}(\phi,\theta)\big)}{\partial\phi}\right|_{\phi=\frac{\pi}{2}} d\theta \tag{37}$$

Implementation technique: final formulation

- **Green's function for the incremental displacement and mean stress fields**:

$$v_k^g(\boldsymbol{x}) = -\frac{Q_{g\alpha}Q_{k\beta}}{8\pi^2 r}\int_0^{2\pi}\tilde{V}_{\alpha\beta}(\theta,\pi/2)\,\mathrm{d}\theta \tag{38}$$

$$\dot{p}^g(\boldsymbol{x}) = \frac{Q_{g\alpha}}{8\pi^2 r^2}\int_0^{2\pi}\left.\frac{\partial\tilde{P}_\alpha(\theta,\phi)}{\partial\phi}\right|_{\phi=\frac{\pi}{2}}\mathrm{d}\theta \tag{39}$$

- **Green's function for the gradient of the incremental displacement field**:

$$v_{k,l}^g(\boldsymbol{x}) = -\frac{Q_{g\alpha}Q_{k\beta}Q_{l\gamma}}{8\pi^2 r^2}\int_0^{2\pi}\left.\frac{\partial\tilde{D}_{\alpha\beta\gamma}(\theta,\phi)}{\partial\phi}\right|_{\phi=\pi/2}\mathrm{d}\theta \tag{40}$$

- Rotation tensor $\boldsymbol{Q}$, defining the representation change between the initial reference system $\{\,\boldsymbol{e}_1,\boldsymbol{e}_2,\boldsymbol{e}_3\,\}$ to the local reference system $\{\,\tilde{\boldsymbol{e}}_1,\tilde{\boldsymbol{e}}_2,\tilde{\boldsymbol{e}}_3\,\}$:

$$[\boldsymbol{Q}] = \frac{1}{r\sqrt{x_1^2+x_2^2}}\begin{bmatrix} rx_2 & x_1x_3 & x_1\sqrt{x_1^2+x_2^2} \\ -rx_1 & x_2x_3 & x_2\sqrt{x_1^2+x_2^2} \\ 0 & -(x_1^2+x_2^2) & x_3\sqrt{x_1^2+x_2^2}\end{bmatrix} \tag{41}$$

Example: force dipole in an axisymmetric infinite prestressed material

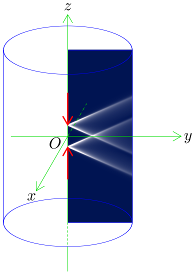

Figure 14: Level sets of $|v_g(\boldsymbol{y})|$ for a force dipole acting on the symmetry axis of an infinite, incompressible, and prestressed J_2-material ($N = 0.4$, $\lambda_z = 0.337$).

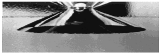

(a) Soda-lime glass.

(b) Shatter cones.

Figure 15: Conical failure.

- Shear moduli within the J_2-flow theory ($\varepsilon_e = |\ln \lambda_z|$, $\sigma = K\varepsilon_e^{N-1} \ln \lambda_z$):

$$\mu_1 = \frac{KN}{3}\varepsilon_e^{N-1}, \quad \mu_2 = \frac{K}{6}(N+1)\varepsilon_e^{N-1}, \quad \mu_3 = \frac{K}{2}\frac{\lambda_z^3+1}{\lambda_z^3-1}\varepsilon_e^{N-1}\ln\lambda_z, \quad W = \frac{K}{N+1}\varepsilon_e^{N+1}. \quad (42)$$

- Shear cones formation is promoted when approaching the elliptic boundary

Conclusions and future developments

- The 2-D inclusion and dislocation problems and the 3-D concentrated force problem have been solved for the case of infinite, anisotropic, homogeneously prestressed and incompressible elastic material.
- By means of the analytical solution for concentrated force, the edge dislocation problem has been numerically solved to investigate the shear band formation, showing that dislocation activity is strongly promoted near the elliptic border.
- Solution for the force dipole shows the formation of failure cones.
- More accurate photoelastic experiments may be performed in order to reconstruct the (deviatoric) stress field from the analysis of the photoelastic fringes.
- The obtained solutions pave the way to investigate the case of 3-D inclusions and dislocations in prestressed materials.

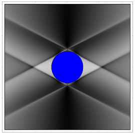

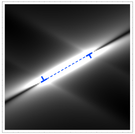

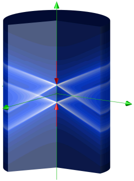

References

- J.D. Eshelby. "The continuum theory of lattice defects". In: *Solid State Phys.* 3.C (1956), pp. 79–144.
- J.D. Eshelby. "The determination of the elastic field of an ellipsoidal inclusion, and related problems". In: *Proc. Royal Soc. A* 241.1226 (1957), pp. 376–396.
- J.D. Eshelby. "A simple derivation of the elastic field of an edge dislocation". In: *British Journal of Applied Physics (B.J.A.P.)* 17.9 (1966), pp. 1131–1135.
- J.R. Willis. "Dislocations and inclusions". In: *J. Mech. Phys. Solids* 13.6 (1965). Ed. by Pergamon Press Ltd., pp. 377–395.
- L.P. Argani, D. Bigoni, and G. Mishuris. "Dislocations and inclusions in prestressed metals". In: *Proc. Roy. Soc. A* 469.2154 (2013).
- V. Volterra. "Sur l' équilibre des corps élastiques multiplement connexes". In: *Annales Scientifiques de l' É.N.S. 3^e série* 24 (1907), pp. 401–517.
- M.A. Biot. *Mechanics of incremental deformations.* New York, NY: John Wiley and Sons, 1965.
- D. Bigoni. *Nonlinear solid mechanics. Bifurcation theory and material instability.* Cambridge, UK: Cambridge University Press, 2012.
- J.W. Hutchinson and K.W. Neale. "Finite strain J_2-deformation theory". In: *Proc. IUTAM Symp. on Finite Elasticity.* Ed. by D. E. Carlson and R.T. Shield. The Hague, The Netherlands: Martinus Nijhoff, 1979, pp. 237–247.
- D. Bigoni and D. Capuani. "Green's function for incremental nonlinear elasticity: shear bands and boundary integral formulation". In: *J. Mech. Phys. Solids* 50.3 (2002), pp. 471–500.
- D. Bigoni et al. "A novel boundary element approach to time-harmonic dynamics of incremental non-linear elasticity: the role of pre-stress on structural vibrations and dynamic shear banding". In: *Comp. Methods Appl. Mech. Eng.* 196.41-44 (2007), pp. 4222–4249.

Special Thanks to the Colleagues and Friends that contributed to this Thesis

Davide Bigoni

Diego Misseroni

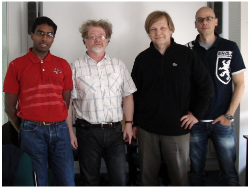

Gennady Mishuris
Alexander B. Movchan
Andrea Piccolroaz

Natasha Movchan
Domenico Capuani

Thank You for Your attention!